Eur. Phys. J. B **49**, 37–45 (2006)
DOI: 10.1140/epjb/e2006-00027-y

THE EUROPEAN PHYSICAL JOURNAL B

# Anomalous magnetoresistance in $[Sr_2Bi_{2-x}Pb_xO_4]^{RS}[CoO_2]_y$ (x = 0, 0.3, and 0.4; y ≈ 1.85) single crystals

X.G. Luo, X.H. Chen[a], G.Y. Wang, C.H. Wang, X. Li, G. Wu, and Y.M. Xiong

Hefei National Laboratory for Physical Science at Microscale and Department of Physics, University of Science and Technology of China, Hefei, Anhui 230026, P.R. China

Received 15 September 2005
Published online 31 January 2006 – 

**Abstract.** Magnetoresistance (MR) of the $[Sr_2Bi_{2-x}Pb_xO_4]^{RS}[CoO_2]_y$ ($x$ = 0, 0.3, and 0.4; $y \approx 1.85$; RS is referred to rocksalt block) single crystals is investigated systematically. A nonmonotonic variation of the isothermal in-plane and out-of-plane MR with the field is observed. The out-of-plane MR is positive at high temperatures and increases with decreasing $T$, and exhibits a pronounced hump, then changes the sign from positive to negative at a certain temperature. These results strongly suggest that the observed MR consists of two contributions: one *negative* and one *positive* component. The isothermal MR in high magnetic fields follows a $H^2$ law. The negative contribution comes from spin scattering of carriers by localized-magnetic-moments based on the Khosla-Fischer model.

**PACS.** 75.47.-m Magnetotransport phenomena; materials for magnetotransport – 71.30.+h Metal-insulator transitions and other electronic transitions – 71.27.+a Strongly correlated electron systems; heavy fermions

## 1 Introduction

The triangular layered cobaltites attracted a great deal of interest for the large thermoelectric power ($S$) with low resistivity ($\rho$) and low thermal conductivity ($\kappa$)(thus the large thermoelectric figure of merit $ZT = S^2T/\rho\kappa$) for the application reasons. A lot of efforts has focused on the enhancement of the figure of merit [1–3]. One important aspect for such effort is to make out why the metallic oxides with triangular $CoO_2$ layers have such unusually large $S$ compared to the conventional metal. Therefore, the work on understanding the fundamental properties of this systems becomes especially significant.

A number of results has been obtained on the transport and magnetic properties of the triangular layered cobaltites, such as Curie-Weiss susceptibility and temperature-dependent Hall coefficient and anomalous magnetoresistance [1,4–8]. Recently, superconductivity was found in one of the promising thermoelectrical compound $Na_xCoO_2$ with $x = 0.35$ by intercalating water molecules into between the $Na^+$ and $CoO_2$ layers [9]. Later, Foo et al. [10] observed an insulating resistivity below 50 K in the composition of $x = 0.5$, which is considered to be related to the strong coupling of the holes and the long-range ordered $Na^+$ ions. The strong magnetic field dependence of $S$ in $Na_xCoO_2$ [11] and $[Bi_{1.7}Co_{0.3}Ca_2O_4]^{RS}[CoO_2]_{1.67}$ [4] provides an unambiguous evidence of strong electron-electron correlation in the triangular layered cobaltites. The large $S$ with metallic resistivity, superconductivity, charge ordering existing with various $x$, displays a complicated and profuse electronic state in $Na_xCoO_2$. This has inspired numerous theoretical and experimental studies on the triangular layered cobaltites.

In this paper, we present new results on the magnetoresistance (MR) of $[Sr_2Bi_{2-x}Pb_xO_4]^{RS}[CoO_2]_y$ ($x$ = 0, 0.3 and 0.4; $y \approx 1.85$) single crystals. The $[Sr_2Bi_{2-x}Pb_xO_4]^{RS}[CoO_2]_y$ possesses a "misfit" crystal structure consisting of the alternating stacks of two subsystems along the $c$-axis: the quadruple $[Sr_2Bi_{2-x}Pb_xO_4]$ rocksalt-like layers and the single $[CoO_2]$ CdI-type layer. "RS" and "$y$" refer to the rocksalt and to the $b_{RS}/b_{CdI}$ ratio of the $b$ incommensurate cell parameters belonging to the two different sublattices. The Pb-free sample, with the exact formula as $[Bi_{0.87}SrO_2]_2^{RS}[CoO_2]_{1.82}$ [12], is paramagnetic down to 2 K [5,14]. With doping by Pb, weak ferromagnetism is induced, which is considered to originate from a canted-antiferromagnetism or to coexist with spin-glass [5,15]. The coexistence of ferromagnetic and antiferromagnetic interaction makes this system intriguing. It has been reported that there exhibits large *negative* MR in $[Ca_2CoO_3]^{RS}[CoO_2]_{1.62}$, $[Sr_2Bi_{2-x}Pb_xO_4]^{RS}[CoO_2]_y$ $[Sr_2Bi_{2-x}Pb_xO_4]^{RS}[CoO_2]_y$, $[Bi_{1.7}Co_{0.3}Ca_2O_4]^{RS}[CoO_2]_{1.67}$, $[Pb_{0.7}A_{0.4}Sr_{1.9}O_{1.9}O_3]^{RS}$

[a] e-mail: chenxh@ustc.edu.cn

$[CoO_2]_{1.8}$ (A = Hg, Co) [1,3–5,13] while *positive* MR in $[Tl_{0.36}Sr_{0.9}O]^{RS}[CoO_2]_{0.89}$, $[Bi_2Ba_{1.8}Co_{0.2}O_4]^{RS}[CoO_2]_2$ and $Na_{0.75}CoO_2$ [6–8]. Very recently, a magnetic-field-induced insulator-to-metal transition was observed by us in oxygen-annealed $[Ca_2CoO_3]^{RS}[CoO_2]_{1.62}$ [13]. Large negative MR is ascribed to suppression of spin scattering [1,3–5]. The positive $H^2$-dependence of MR in $Na_{0.75}CoO_2$ is attributed to conventional orbital motion of carriers [8], while linear positive MR in $[Bi_2Ba_{1.8}Co_{0.2}O_4]^{RS}[CoO_2]_2$ is interpreted in an opening of pseudogap [7]. Up to now, the unusual MR is not well understood entirely yet. Further detailed investigation is required to describe the physical nature of these triangular layered cobaltites. For the easy control of doping level, $[Sr_2Bi_{2-x}Pb_xO_4]^{RS}[CoO_2]_y$ ($x$ = 0, 0.3, and 0.4; $y \approx 1.85$) single crystals are chosen to be studied systemically. In the present article, the magnetoresistance, measured in in-plane and out-of-plane configurations with the fields up to 13.5 T, exhibits nonmonotonic field-dependent behavior. The MR shows a complicated dependence of the field and temperature. Its magnitude is enhanced initially with increasing $H$, and reaches a maximum at a certain field. The out-of-plane MR is positive at high temperatures, and shows a pronounced hump with decreasing $T$. These results suggest the MR comes from the contribution of *negative* and *positive* components, which is strongly dependent of temperature and field.

## 2 Experiment

The $[Sr_2Bi_{2-x}Pb_xO_4]^{RS}[CoO_2]_y$ ($x$ = 0, 0.3, and 0.4; $y \approx 1.85$) single crystals were grown by a self-flux method. High-purity $Bi_2O_3$, PbO, $SrCO_3$ and $Co_3O_4$ were mixed with a nominal mole ratio of Bi:Pb:Sr:Co = 2-$x$:$x$:2:2 ($x$ = 0, 0.5 and 0.6) and preheated at 800 °C for 24 h. Additional $Bi_2O_3$ as the flux was mixed with the obtained precursors carefully. The mixture was melt at 1050 °C for 2 h, and followed a slow cooling procedure with a cooling rate of 4–5 °C/h to 800 °C, then cooled by furnace. Platelike crystals were easily cleaved from the melt. The actual composition Bi:Pb:Sr:Co for the crystals with the nominal composition of $x$ = 0, 0.5 and 0.6 was determined by inductively coupled plasmas (ICP) atomic emission spectroscopy to be 2.02:0:2:1.91, 1.68:0.30:2:1.89, and 1.54:0.41:2:1.83, respectively.

The measurements of in-plane and out-of-plane resistivity with a configuration described in reference [16] were performed using the standard ac six-terminal method with the frequency of excitation current to be 15.9 Hz and the magnitude of excitation voltage 6 mV. It has been reported that there exists a large anisotropy in $[Sr_2Bi_{2-x}Pb_xO_4]^{RS}[CoO_2]_y$ [5]; so just a tiny fraction of the c-axis transport can badly contaminate an *ab*-plane measurement and lead to a large inconsistency in the observed ratio. In order to check for the *c*-axis transport contaminating the *ab*-plane measurement, a six terminal measurement was used in this study. To ensure a homogeneous current flow in the sample, for the ab-plane measurements, the current contacts were attached to the two side faces of the plate samples. For the *c*-axis measurements, six contacts were attached to the two surfaces. Single crystals were cut into a rectangular shape with a typical dimension of 1.0 × 0.5 × 0.05 mm$^3$ and 1.0 × 1.0 × 0.05 mm$^3$ for the measurement of in-plane and out-of-plane resistivity, respectively. The magnetic field was supplied by a superconducting magnet system (Oxford Instruments). Magnetic susceptibility measurement was carried out with a superconducting quantum interference device (SQUID) magnetometer (MPMS-7XL, Quantum Design).

## 3 Experimental results and discussion

### 3.1 Transport properties

Figure 1a shows the temperature dependence of the in-plane resistivity ($\rho_{ab}(T)$) of the samples with $x$ = 0, 0.3, and 0.4. The crystals show metallic behavior at high temperatures. $\rho_{ab}(T)$ exhibits a minimum at 140 K for the sample with $x$ = 0, 70 K for the sample with $x$ = 0.3, and 45 K for the sample with $x$ = 0.4, respectively. Below this temperature the crystals show a diverging resistivity. The resistivity and the temperature corresponding to the minimum resistivity decrease with increasing the content of the Pb substitution for Bi. The ratio $\rho_{ab}(T = 4\,\mathrm{K})/\rho_{ab}(T = 300\,\mathrm{K})$ also decreases with enhancing the doping level of Pb. These indicate that the Pb doping induces holes into the system. These results are consistent with the previous report [5]. Figure 1b shows the temperature dependence of the out-of-plane resistivity ($\rho_c(T)$) of the samples. For the samples with $x$ = 0 and $x$ = 0.3, $\rho_c(T)$ shows insulator-like behavior in the whole temperature range. It increases slightly above about 50 K and enhances suddenly below 50 K with decreasing temperature. For the sample with $x$ = 0.4, $\rho_c(T)$ shows an insulator-like behavior above 100 K and below 100 K it shows a metallic behavior ($\mathrm{d}\rho_c/\mathrm{d}T > 0$). With further decreasing temperature down to 30 K, $\rho_c(T)$ shows a reentrant insulating behavior and increases sharply with decreasing temperature. It shows a broad maximum at $T_\mathrm{M} \approx 100$ K. Such a broad maximum is very similar to that observed in $(Bi_{0.5}Pb_{0.5})_2Ba_3Co_2O_y$ ($T_M \approx 200$ K) and $NaCo_2O_4$ ($T_M \approx 180$ K), where it is thought to be an incoherent-coherent resistivity transition [17]. This transition was considered as a crossover in the number of effective dimension from two to three [17]. The diverging resistivity at the low temperatures has been attributed to the decrease of the effective carrier number $n_\mathrm{c}$ due to a pseudogap formation below 30–50 K [18]. In addition, the Hall coefficient was reported to exhibit a sudden enhancement [5,19], suggesting a reduction of $n_\mathrm{c}$ at low temperatures. Another point of view is that the resistivity upturn and the sudden enhancement of Hall coefficient below 50 K are associated with the magnetic ordering in low $T$ [6].

Figure 1c shows the temperature dependence of the anisotropy $\rho_c/\rho_{ab}$ for the three samples. The three samples show close values of the anisotropy. The anisotropy shows a weak temperature dependence above 50 K for the all three samples, and increases sharply below 30 K.

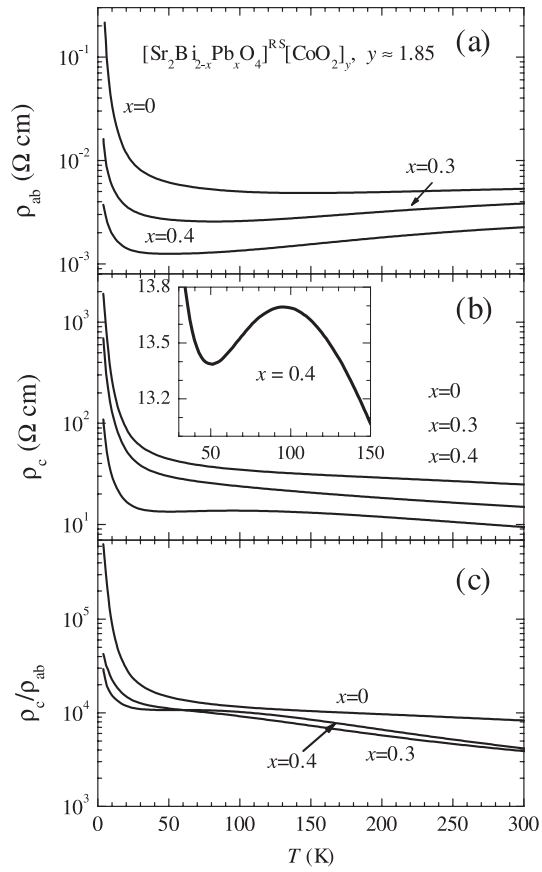


**Fig. 1.** The temperature dependence of in-plane (a), out-of-plane (b) resistivity and the anisotropy $\rho_c/\rho_{ab}$ (c) for three samples with $x = 0$, 0.3 and 0.4.

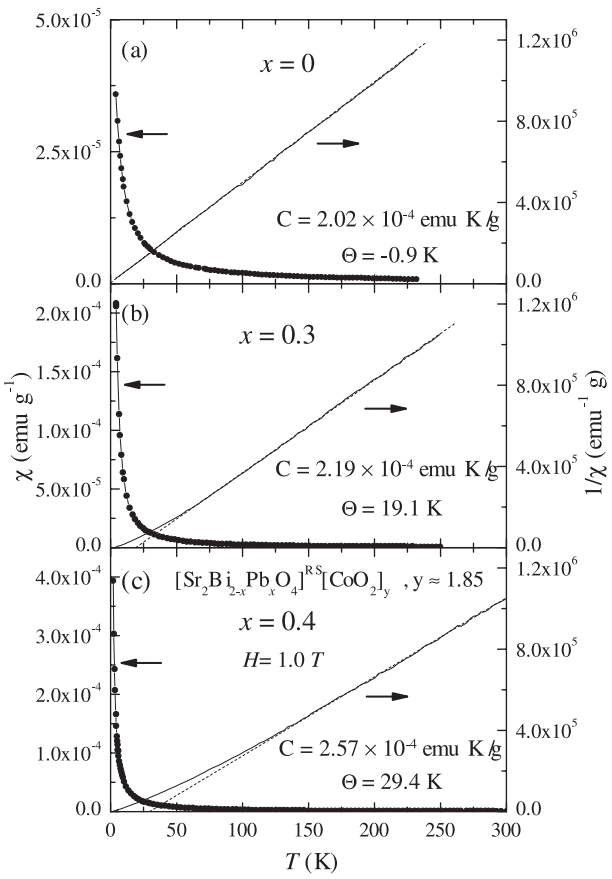


**Fig. 2.** The temperature dependence of the magnetic susceptibility and inverse susceptibility of the three samples. The magnetic field is applied perpendicular to the *ab* plane. The dash lines correspond to Curie-Weiss behavior.

It is addressed that the anisotropy for the sample with $x = 0.4$ saturates below 100 K, which coincides with the "incoherent-coherent" transition temperature. The temperature-independent anisotropy between 100 and 30 K and the peak in $\rho_c(T)$ for the sample with $x = 0.4$ sample give evidence for existence of the dimensional crossover from two to three. In order to make clear the physics of the diverging resistivity and "incoherent-coherent" transition, it requires angle-resolved photoemission to determine the electronic structure.

### 3.2 Magnetic properties

Figure 2 shows the temperature dependence of magnetic susceptibility under the magnetic field of 1T for the three samples. In previous reports [5,15], $[Sr_2Bi_{2-x}Pb_xO_4]^{RS}[CoO_2]_y$ with large Pb content shows a magnetic transition at low temperature. In Figure 2, no obvious magnetic transition is observed down to 2 K for all crystals. The dash lines correspond to the fitting of the linear part of the data for all samples with Curie-Weiss law,

$$1/\chi = (T - \Theta)/C \qquad (1)$$

where $C$, $\Theta$ are Curie constant and Weiss temperature, respectively. The inverse susceptibility indicates paramagnetic behavior for the sample with $x = 0$ down to 2 K with a very small negative $\Theta$. With increasing Pb doping level, $\Theta$ becomes positive and its magnitude increases, indicative of the appearance of ferromagnetic correlation. $C$ also increases with increasing Pb content, suggesting the enhancement of the effective moment of Co ions. The samples with $x = 0.3$ and 0.4 show Curie-Weiss behavior at high temperatures with positive $\Theta$, and deviates from Curie-Weiss law below 60 and 125 K, respectively. This reveals the presence of a short-range ferromagnetic order, which is consistent with the positive $\Theta$. These results are in good agreement with the previous report [5].

### 3.3 Magnetoresistance

Figure 3 shows the evolution of $\Delta\rho_{ab}/\rho_{ab}$ and $\Delta\rho_c/\rho_c$ ($\Delta\rho/\rho = ((\rho(H) - \rho(0))/\rho(0))$ with varying temperature at the field of 13.5 T. Above 12 K, the in-plane MR for the sample with $x = 0$ is very small and negative, and its magnitude increases sharply below 12 K with decreasing temperature. The negative MR reaches 37% at 4 K. The in-plane MR is negative and its magnitude monotonously increases with decreasing temperature, and reaches 33%,

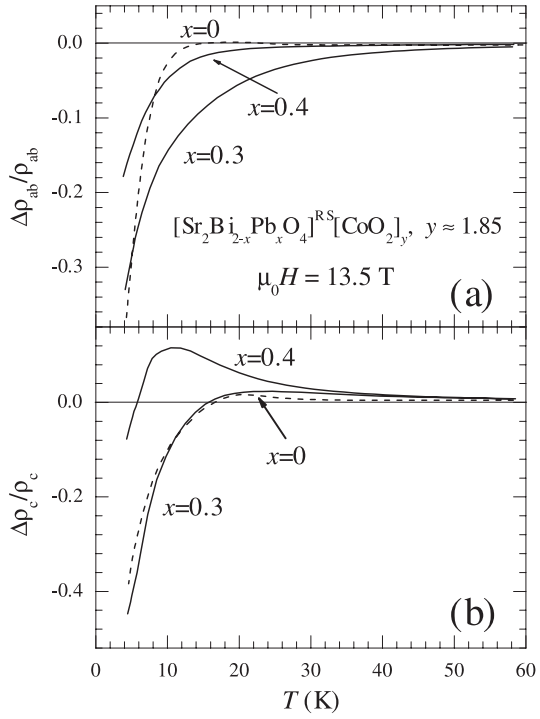


**Fig. 3.** The in-plane (a) and out-of-plane (b) magnetoresistance as a function of temperature at 13.5 T for the three samples. The field is applied along the *c*-axis.

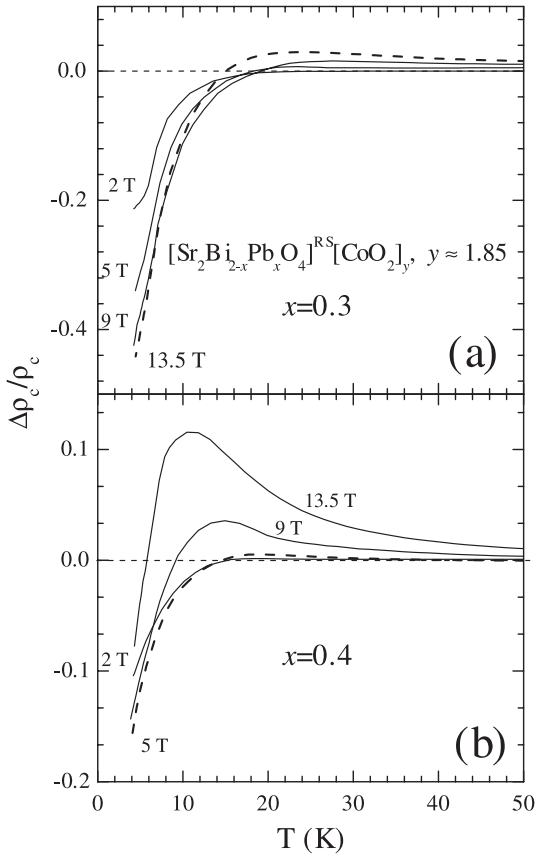


**Fig. 4.** The out-of-plane magnetoresistance as a function of temperature at various magnetic fields for the samples with $x = 0.3$ (a) and $x = 0.4$ (b). The field is applied along the *c*-axis.

and 18% at 4 K for the samples with 0.3 and 0.4, respectively. However, the out-of-plane MR shows anomalous features compared to the in-plane MR. The out-of-plane MR is positive at high temperatures for the samples. The MR first increases with decreasing temperature, and exhibits a broad hump. With further decreasing temperature, the MR changes the sign from positive to negative, and its magnitude begins to increase sharply.

In order to understand the anomalous behavior in out-of-plane MR, it was systematically studied in the different magnetic fields. The out-of-plane MR for the samples with $x = 0.3$ and 0.4 as a function of temperature at various magnetic fields is shown in Figure 4. The MR is positive at high temperatures as observed in Figure 3, and increases monotonically with increasing magnetic field. Broad humps of the positive MR can be observed at all magnetic fields for the two samples. The position of the humps shifts to lower temperature with enhancing magnetic field. With further decreasing $T$, the MR becomes negative at low temperatures. The temperature for the MR passing through zero decreases monotonously with increasing the field. The negative MR exhibits complex behavior at various fields. The magnitude of MR for the sample with $x = 0.3$ varies with field monotonically at 4 K, while in the temperature range from 8 K to 18 K, it increases firstly as field increased to 9 T and then decreases as field is higher than 9 T at all temperatures. The magnitude of MR for the sample with $x = 0.4$ reaches maximum around 5 T at 4 K. These results suggests that the observed MR comes from two contributions, i.e. one *negative* and one *positive* contribution to the total MR. At high temperatures, the positive component is predominant, while the negative component grows more rapidly than the positive one with decreasing $T$ and MR has a negative value in low temperatures.

In order to clearly understand the complicated behavior shown in Figure 4, isothermal MR is studied by sweeping the fields up to 13.5 T at different temperatures. Figure 5 shows the isothermal in-plane MR at 5, 15 and 40 K for the samples with $x = 0$, 0.3, and 0.4. There are some salient features of the MR. (I) The MR at 40 K and 15 K for the crystal with $x = 0$ first increases with increasing field, and reaches a maximum at 4 T (for both of the temperatures), then decreases monotonically. (II) All the other MR is negative. The magnitude of these MR increases monotonically with increasing magnetic field except that at 15 K in the sample with $x = 0.4$. (III) The magnitude of the MR at 15 K for the sample with $x = 0.4$ first increases with increasing magnetic field, and reaches a maximum ($\sim$10%) at 11.4 T, then decreases with further increasing field (see the inset in Fig. 5b). It suggests the presence of a positive contribution in additional to the negative MR in this case. Such an anomalous MR has not been observed in triangular layered cobaltites previously. Only large monotonic negative MR has been found in $[Sr_2Bi_{2-x}Pb_xO_4]^{RS}[CoO_2]_y$,

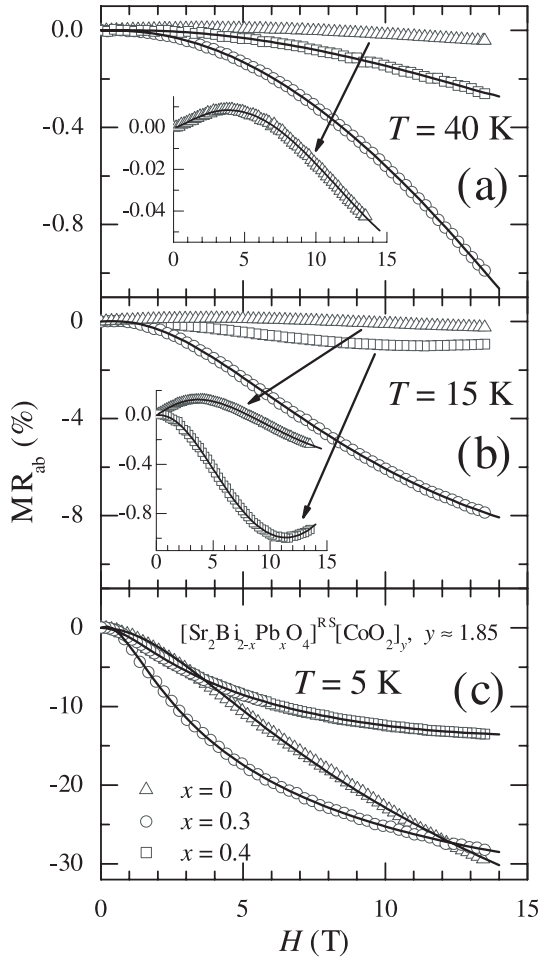


**Fig. 5.** The isothermal in-plane magnetoresistance as function of magnetic field at 40 K, 15 K, and 5 K for the samples with $x = 0$ (△), $x = 0.3$ (○) and $x = 0.4$ (□), where MR = $[\rho(H) - \rho(0)]/\rho(0) \times 100\%$, the subindex ab is referred to the in-plane case. The solid lines are the data fitted by using equation (1). The field is applied along the $c$-axis.

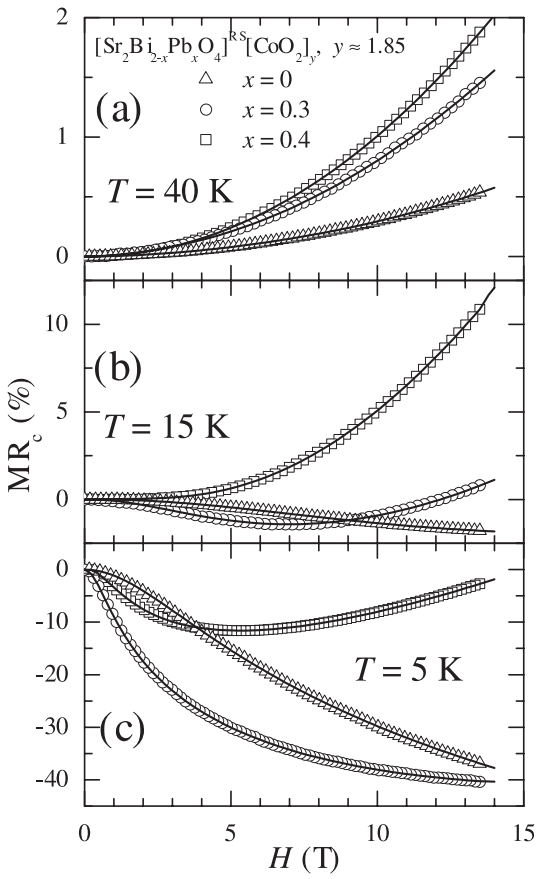


**Fig. 6.** The isothermal out-of-plane magnetoresistance as function of magnetic field at 40 K, 15 K, and 5 K for the samples with $x = 0$ (△), $x = 0.3$ (○) and $x = 0.4$ (□). The subindex c of MR is referred to the out-of-plane configuration. The solid lines represent the data fitted by equation (1). The field is applied along the $c$-axis.

$[Bi_{1.7}Co_{0.3}Ca_2O_4]^{RS}[CoO_2]_{1.67}$ up to 9 T [4,5] and $[Ca_2CoO_3]^{RS}[CoO_2]_{1.62}$ up to 14 T [13]. (IV) The crystal with $x = 0.3$ have the largest negative MR for all temperature except that above 12 T at 5 K. This is consistent with the data shown in Figure 3a, where an intersection is observed at about 5.1 K in MR curves for the samples with $x = 0$ and $x = 0.3$. According to the susceptibility (Fig. 2) and $\mu$SR measurements [5,14], the Pb-free crystal is almost paramagnetic down to 2 K. Ferromagnetism would be induced by Pb doping and the transition temperature ($T_c$) increases with increasing Pb doping level, with $T_c = 3.2$ K for $x = 0.44$ and 5 K for $x = 0.51$, respectively [5]. Thus in the present samples, the $T_c$ is less than 3.2 K and beyond our measurement temperature range. Actually, no obvious magnetic transition is observed down to 2 K in Figure 2. The relative large magnitude of the negative MR at 15 K and 5 K seems to suggest the presence of short-range ferromagnetic order far above $T_c$, because ferromagnetic fluctuation due to short-range order could be suppressed by magnetic field and give rise to negative MR. However, the sample with $x = 0$ shows paramagnetic behavior down to 2 K, which does not support that the negative MR arises from the presence of short-range ferromagnetic order. New scenario is required to interpret the large negative MR in this system.

In Figure 5b, the nonmonotonic field-dependence of MR is anomalous for triangular layered cobaltites, which has not been observed previously in these systems. Such a nonmonotonic MR is more obvious in the out-of-plane MR. Figure 6 shows the evolution of the isothermal out-of-plane MR with magnetic field along the $c$-axis at 5, 15, and 40 K for the three samples. The MR is positive at 40 K for all the samples (in contrast to the in-plane MR), and increases with increasing Pb doping level. The MR at 15 K is positive for the sample with $x = 0.4$, while negative for the Pb-free crystal. These two samples exhibit monotonic MR at 15 K. On the contrary, the MR for the sample with $x = 0.3$ at 15 K is first negative and its magnitude increases with increasing magnetic field, and reaches a maximum (∼1.43%) at about 6.9 T, then decreases and passes through zero at 12.5 T. The MR at 5 K is negative for all the crystals. In Figure 6c, the MR at 5 K for the

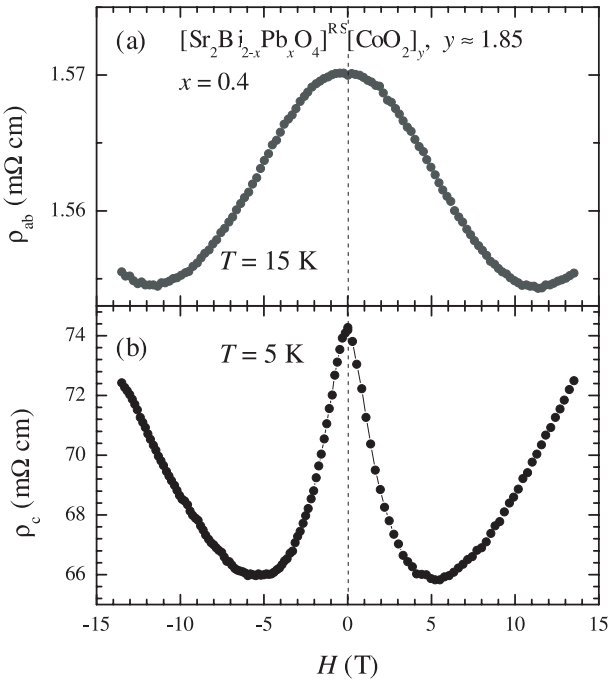


**Fig. 7.** (a) The in-plane ($T$ = 15 K) and (b) out-of-plane ($T$ = 5 K) isothermal MR with the magnetic field varying from −13.5 T to 13.5 T for the sample with $x = 0.4$.

samples with $x = 0$ and 0.3 increases monotonically with increasing $H$, while the MR of the sample with $x = 0.4$ exhibits an analogous behavior to that of the sample with $x = 0.3$ at 15 K, the magnitude of MR first increases with enhancing $H$, and reaches a maximum (∼11.6%) around 5.3 T, then decreases. The above results are well consistent with the evolution of magnetoresistivity with temperature in Figure 4. It should be pointed out that for the sample with $x = 0.4$ the positive MR at 15 K is larger than that at 40 K, which is consistent with the hump observed in Figure 4. The results above strongly suggest *the presence of a positive contribution in MR*. It should be mentioned that a rapid increase of Hall voltage was observed in $[Sr_2Bi_{2-x}Pb_xO_4]^{RS}[CoO_2]_y$ below 50 K [5,15], which may contaminate the MR signal. In order to check it, we measured the MR with the fields from −13.5 T to 13.5 T, which is shown in Figure 7 for the typical sample with $x = 0.4$. In Figure 7, the in-plane (15 K) and out-of-plane MR (5 K) show the almost same value at $-H$ and $+H$. Considering that MR is usually symmetric with $H$, while the Hall resistivity is antisymmetric with $H$, the same MR at $-H$ and $+H$ indicates that the unusual upturn MR doesn't contain the contamination of Hall effect.

## 3.4 The possible origin of the anomalous MR

In order to understand the complicated MR, an expression consisting of negative and positive contributions for MR could be used to describe the anomalous nonmonotonic MR. It is found that all the isothermal MR can be well fitted by the following expression:

$$\frac{\Delta\rho}{\rho} = -A_1^2 \ln(1 + A_2^2 H^2) + B_1^2 H^n, \qquad (2)$$

where $A_1$, $A_2$, $B_1$, and $n$ are variable parameters for fitting. The fitted data are plotted in Figures 5 and 6 by solid lines. One can find that all the isothermal MRs are well fitted.

### 3.4.1 The negative component

The first term in equation (1) comes from a semiempirical expression proposed by Khosla and Fischer [20] and has been previously used to explain the negative MR observed in $n$-type CdS [20], $n$-type Si [21] and (In, Mn)As semiconductors [22]. The basis for this formula is Toyazawa's localized-magnetic-moment model of magnetoresistance, where carriers in an impurity band are scattered by the localized spin of impurity atoms [23]. It is derived from third-perturbation expansion of the $s$–$d$ exchange Hamiltonian in this local-magnetic-moment model of Toyazawa [20,23]. Well agreement of the observed MR with the equation (1) reflects that the negative MR comes from the interaction between conducting carriers and localized magnetic moments, and it reveals a decrease of spin-dependent scattering of carriers in magnetic field. This model requires a separation of conducting carriers and localized magnetic moments in a semiconductor. According to the photoemission and X-ray-absorption spectroscopy measurements in the misfit-layered $[Sr_2Bi_{2-x}Pb_xO_4]^{RS}[CoO_2]_y$ [24], both $Co^{3+}$ and $Co^{4+}$ have low spin configuration. The electrons of $Co^{3+}$ and $Co^{4+}$ locate in the $t_{2g}$ orbitals, and the three-folded $t_{2g}$ orbitals are split into one $a_{1g}$ subband and two $e'_g$ subbands due to the rhombohedral crystal field [25]. In reference [24], it has been pointed out that holes locate mainly in the $a_{1g}$ subband, which are strongly coupled to the lattice and become localized holes. A minority of holes locate in the $e'_g$ subbands. The former are "heavier" than the latter. The local magnetic moments are attributed to the $a_{1g}$ holes [5] due to the strong electron-phonon coupling while $e'_g$ holes is conducting carriers responsible for the relative low resistivity. Therefore, it is inferred that the conducting carriers formed by the $e'_g$ holes interact with the localized magnetic moments from the $a_{1g}$ holes through $s$–$d$ exchange. Actually, such anomalous MR with nonmonotonic field dependence as shown in Figure 6 has been previously observed in $R_2Ni_2Si_5$ (R = Pr, Dy, Ho, and Er) compounds, which was attributed to the presence of short-range ferromagnetic order in the literatures [26,27]. However, in the Pb-free crystal, our data and previous reports [5,14] indicate paramagnetic magnetism down to 2 K. Therefore, it seems to be difficult to be understood by the presence of short-range ferromagnetic order. Using Khosla-Fischer model with $s$–$d$ exchange in localized-magnetic-moment model, the negative MR in the semiconducting region for these crystals may be well understood.

In previous reports [5], only monotonic behavior of the negative in-plane MR is observed in $[Sr_2Bi_{2-x}Pb_xO_4]^{RS}[CoO_2]_y$ system as $H \leq 9T$. However, in the present work, a maximum in magnitude is observed at about 11.4 T for the sample with $x = 0.4$. More pronounced nonmonotonic behavior is observed in the out-of-plane MR. It is clear that there exist both *negative* and *positive* contributions to the MR, which cause the anomalous behavior of MR. The negative component comes from the suppression of the carrier-spin scattering in magnetic field, just as that in $[Ca_2CoO_3]^{RS}[CoO_2]_{1.62}$, $[Bi_{1.7}Co_{0.3}Ca_2O_4]^{RS}[CoO_2]_{1.67}$, $[Pb_{0.7}A_{0.4}Sr_{1.9}O_{1.9}O_3]^{RS}[CoO_2]_{1.8}$ (A = Hg, Co) etc. [1,3–5,13]. We have attributed it to the suppression of the localized-magnetic-moment scattering from $a_{1g}$ holes to the itinerant $e'_g$ holes. In (In, Mn)As the nearly free s electrons are scattered by the magnetic moment of Mn [28]. Yamamoto et al. found that the anomalous Hall coefficient in $[Sr_2Bi_{2-x}Pb_xO_4]^{RS}[CoO_2]_y$ can scale with resistivity by the same power law as in (In, Mn)As, and they considered that there could also exist itinerant elections scattered by localized magnetic moments [19]. Recently, the low-temperature negative MR in (In, Mn) As was described by the Khosla-Fischer model [22]. In the present paper, the same fitting for negative component of MR can be used, and it demonstrates that the negative MR in $[Sr_2Bi_{2-x}Pb_xO_4]^{RS}[CoO_2]_y$ really results from the suppression of spin-scattering of carriers in the Khosla-Fischer model. It should be mentioned that the isothermal MR at 6 K and 17 K in $[Ca_2CoO_3]^{RS}[CoO_2]_{1.62}$ can also be fitted by the first term in equation (1) [29]. This seems to suggest that the negative MR observed in the triangular layered cobaltite can be universally described by the Khosla-Fischer model.

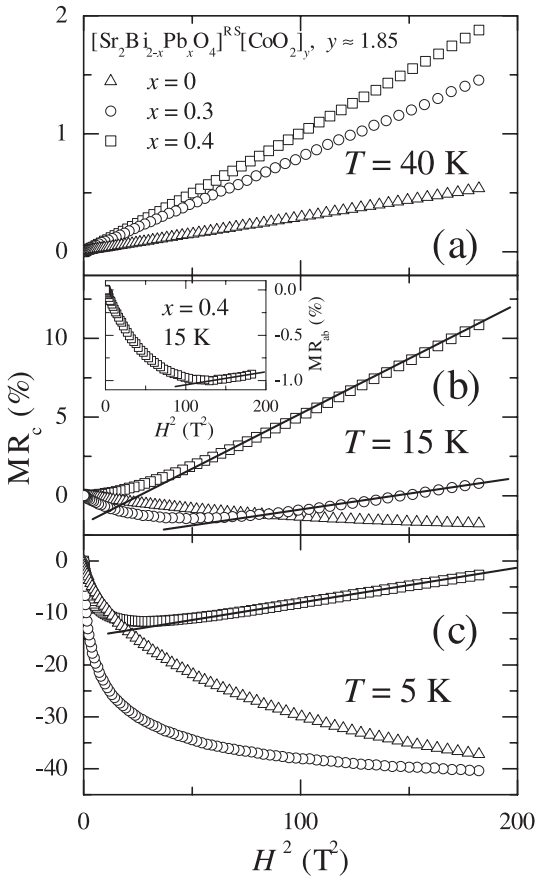


**Fig. 8.** The square magnetic dependence of the isothermal out-of-plane MR at 5, 15, and 40 K for the crystals with $x = 0$ (△), $x = 0.3$ (○) and $x = 0.4$ (□). The inset shows the in-plane MR at 15 K for $x = 0.4$. The field is applied along the $c$-axis.

### 3.4.2 Positive component

Therefore, the anomalous behavior of MR seems to come from the positive component. The hump feature in the out-of-plane MR vs. $T$ curves and the nonmonotonic isothermal MR strongly suggest the presence of the positive contribution in addition to the negative component. The second term in equation (1) gives the positive component of MR, which is proportional to $H^n$, with $n$ varying from 0.77 to 2.19. It is found that $n$ is ranging from 1.8 to 2.19 for the MR data with a upturn behavior, while the rather smaller values of $n$ are obtained for the negative MR with monotonic behavior. A similar $H$ power law has been used by Roth et al. to explain the MR behavior in heavily doped Ge and Si [30]. But this unusual term is not well understood yet. The nonmonotonic MR found in $R_2Ni_2Si_5$ (R = Pr, Dy, Ho, and Er) is almost linear to $H$ in high fields [26,27], which is ascribed to the blocks structure [26]. As a contrast, a power law dependence of the positive component with power exponent dependent dramatically of $T$ and sample is observed in our case. The unusual $H$ power law magnetoresistance seems hard to be understood.

We compare the positive component with the positive MR observed in the other triangular layered cobaltites. Large positive MR has ever been observed in $Na_{0.75}CoO_2$ and $[Bi_2Ba_{1.8}Co_{0.2}O_4]^{RS}[CoO_2]_2$ [7,8], and is proportional to $H^2$ in the former, while nearly linear to $H$ in the latter. In order to understood unusual positive component in MR, the out-of-plane MR is plotted in Figure 8 by $H^2$ scales. It is intriguing that the upturn MR in high fields exhibits a clear $H^2$ behavior. In the inset of Figure 8b, the in-plane MR at 15 K for the sample with $x = 0.4$ also shows almost $H^2$ behavior in high fields. It suggests that in high fields the upturn MR is actually proportional to $H^2$. Figure 9 shows the transverse and longitudinal out-of-plane MR plotted against $H^2$. The $H^2$ dependence in high field can be clearly observed for all the curves. At each temperature, the transverse MR is larger than longitudinal one in high fields. The $H^2$ dependence of positive MR in $Na_{0.75}CoO_2$ was attributed to the conventional orbital motion of carriers [8]. The increase of MR with decreasing temperature in $Na_{0.75}CoO_2$ is accompanying with a dramatic enhancement in carrier mobility. However, in the present crystals, for example, for the sample with $x = 0.4$ the magnitude of $H^2$ term in the out-of-plane MR increases with decreasing temperature from 40 K to

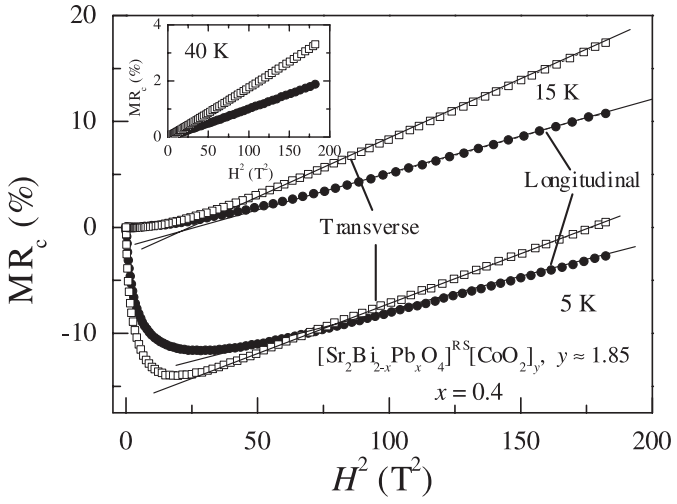


**Fig. 9.** The square magnetic field dependence of the isothermal transverse (□) and longitudinal (•) out-of-plane MR at 5, 15, and 40 K (the inset) for the crystal with $x = 0.4$. Transverse and longitudinal configurations correspond to the field applied within the ab-plane and along the *c*-axis, respectively.

15 K, while the semiconducting resistivity suggests a reduction of mobility of carriers, which is in contrast to the case in $Na_{0.75}CoO_2$ [8]. Nevertheless, it is noteworthy that as the metallicity is enhanced with increasing Pb content, the positive component of MR increases. This seems to be analogous to the evolution of positive MR with decreasing temperature in $Na_{0.75}CoO_2$. Moreover, we note that Sales et al. [31] observed a $H^2$ behavior of longitudinal out-of-plane MR and transverse in-plane MR in $Na_{0.75}CoO_2$ single crystal. Consequently, the positive component of MR in the present study could be attributed to the influence of the Lorentz force on the conduction carriers as well as that in $Na_{0.75}CoO_2$.

It may be possibly associated with the complex magnetic structure in this system. Two possible magnetic configurations have been proposed by Yamamoto et al. [5,15], (1) A canted antiferromagnetic spin structure; and (2) the coexistence of spin-glass and ferromagnetism, to interpret the weak ferromagnetism in Pb-doped crystals. In these two pictures, antiferromagnetic interaction is necessary. A positive MR with a slope following a $H^2$ law can be expected for antiferromagnetic correlation [32]. The presence of AF interactions over the length of the mean free path would lead to a significant positive MR. More microscopic information (such as Co-NMR and neutron scattering data) and theoretical work are required to understand this anomalous nonmonotonic MR.

Finally, we give a comment on the MR behavior of the triangular layered cobaltites with quadruple rocksalt-like layers, $[Bi_{1.7}Co_{0.3}Ca_2O_4]^{RS}[CoO_2]_{1.67}$, $[Sr_2Bi_{2-x}Pb_xO_4]^{RS}[CoO_2]_y$, and $[Bi_2Ba_{1.8}Co_{0.2}O_4]^{RS}[CoO_2]_2$. In these compounds, $[Bi_{1.7}Co_{0.3}Ca_2O_4]^{RS}[CoO_2]_{1.67}$ is the most semiconducting system and shows largest negative MR at low temperature (−87% in 7 T at 2.5 K) [4]. While the most metallic system, $[Bi_2Ba_{1.8}Co_{0.2}O_4]^{RS}[CoO_2]_2$, exhibits large positive MR (11% in 7 T at 2.5 K) [7]. Therefore, it seems naturally to consider the existence of positive component of MR in $[Sr_2Bi_{2-x}Pb_xO_4]^{RS}[CoO_2]_y$, which acts as a moderate system between $[Bi_{1.7}Co_{0.3}Ca_2O_4]^{RS}[CoO_2]_{1.67}$ and $[Bi_2Ba_{1.8}Co_{0.2}O_4]^{RS}[CoO_2]_2$, as a result of the enhancement of metallicity. This is just consistent with the change of the MR with the enhancement of metallicity as Pb content increases. The decrease of the negative MR from Ca compound to Ba compound may also be associated with the enhancement of the metallicity. Consequently, we prefer to take the influence of Lorentz force on the conduction carriers as the origin of the unusual positive component in MR. Alike experiments on $[Bi_{1.7}Co_{0.3}Ca_2O_4]^{RS}[CoO_2]_{1.67}$ and $[Bi_2Ba_{1.8}Co_{0.2}O_4]^{RS}[CoO_2]_2$ single crystals should be carried out to acquire more data to understand the unusual positive MR. Such efforts are performed by us now.

## 4 Conclusion

We have observed an anomalous nonmonotonic field-dependent behavior of MR in $[Sr_2Bi_{2-x}Pb_xO_4]^{RS}[CoO_2]_y$ ($x = 0$, 0.3 and 0.4, $y = \approx 1.85$) single crystals. The MR exhibits a positive hump at high temperatures, following a negative behavior at low temperature, and the magnitude of the negative MR at low temperatures exhibits a maximum with magnetic field. These results strongly suggest that the MR comes from two contribution: one negative and one positive component. The *negative* component is described by the third-perturbation expansion of the *s-d* exchange Hamiltonian in localized-magnetic-moment model of Toyazawa. The *positive* contribution follows a $H^2$ law in high fields. The understanding of this anomalous nonmonotonic MR requires further experimental and theoretical work on the microscopic mechanisms.

This work is supported by the grant from the Nature Science Foundation of China and by the Ministry of Science and Technology of China, and the Knowledge Innovation Project of Chinese Academy of Sciences.

## References

1. A.C. Masset, C. Michel, A. Maignan, M. Hervieu, O. Toulemonde, F. Studer, B. Raveau, J. Hejtmanek, Phys. Rev. B **62**, 166 (2000)
2. G.J. Xu, R. Funahashi, M. Shikano, I. Matsubara, Y.Q. Zhou, Appl. Phys. Lett. **80**, 3760 (2002)
3. D. Pelloquin, A. Maignan, S. Hebert, C. Martin, M. Hervieu, C. Michel, L.B. Wang, B. Raveau, Chem. Mater. **14**, 3100 (2002)
4. A. Maignan, S. Hebert, M. Hervieu, C. Machel, D. Pelloquin, D. Khomskii, J. Phys.: Condens. Matter **15**, 2711 (2003)
5. T. Yamamoto, K. Uchinokura, I. Tsukada, Phys. Rev. B **65**, 184434 (2002)
6. S. Hebert, S. Lambert, D. Pelloquin, A. Maignan, Phys. Rev. B **64**, 172101 (2001)
7. M. Hervieu, A. Maignan, C. Michel, V. Hardy, C. Creon, B. Raveau, Phys. Rev. B **67**, 045112 (2003)

8. T. Motohashi, R. Ueda, E. Naujalis, T. Tojo, I. Terasaki, T. Atake, M. Karppinen, H. Yamauchi, Phys. Rev. B **67**, 064406 (2003)
9. K. Takada, H. Sakurai, E. Takayama-Muromachi, F. Izumi, R.A. Dilanian, T. Sasaki, Nature **422**, 53 (2003)
10. M.L. Foo, Y.Y. Wang, S. Watauchi, H.W. Zandbergen, T. He, R.J. Cava, N.P. Ong, Phys. Rev. Lett. **92**, 247001 (2004)
11. Y.Y. Wang, N.S. Rogado, R.J. Cava, N.P. Ong, Nature **423**, 425 (2003)
12. H. Leligny, D. Grebille, O. Perez, A.C. Masset, M. Hervieu, C. Michel, B. Raveau, C. R. Sci. Paris IIc, Chim. **2**, 409 (1999); H. Leligny, D. Grebille, O. Perez, A.C. Masset, M. Hervieu, C. Michel, B. Raveau, Acta Crystallogr., Sect. B: Struct. Sci. **56**, 173 (2000)
13. X.G. Luo, X.H. Chen, G.Y. Wang, C.H. Wang, Y.M. Xiong, H.B. Song, H. Li, X.X. Lu, e-print `arXiv:cond-mat/0412298`
14. J. Sugiyama, J.H. Brewer, E.J. Ansaldo, H. Itahara, T. Tani, M. Mikami, Y. Mori, T. Sasaki, S. Hebert, A. Maignan, Phys. Rev. Lett. **92**, 17602 (2004)
15. I. Tsukada, T. Yamamoto, M. Takagi, T. Tsubone, Jpn J. Appl. Phys. **39**, 6658 (2000)
16. C.H. Wang, L. Huang, L. Wang, Y. Peng, X.G. Luo, Y.M. Xiong, X.H. Chen, Supercond. Sci. Technol. **17**, 469 (2004)
17. T. Valla, P.D. Johnson, Z. Yusof, B. Wells, Q. Li, S.M. Loureiro, R.J. Cava, M. Mikami, Y. Mori, M. Yoshimura, T. Sasaki, Nature **417**, 627 (2002)
18. T. Itoh, I. Terasaki, Jpn J. Appl. Phys. **39**, 6658 (2000)
19. T. Yamamoto, I. Tsukada, M. Takagi, T. Tsubone, K. Uchinokura, J. Magn. Magn. Mater. **226–230**, 2031 (2001)
20. R.P. Khosla, J.R. Fischer, Phys. Rev. B **2**, 4084 (1970)
21. R.P. Khosla, J.R. Fischer, Phys. Rev. B **6**, 4073 (1972)
22. S.J. May, A.J. Blattner, B.W. Wessels, Phys. Rev. B **70**, 073303 (2004)
23. Y. Toyazawa, J. Phys. Soc. Jpn **17**, 986 (1962)
24. T. Mizokawa, L.H. Tjeng, P.G. Schultze, G.A. Sawatzky, N.B. Brooks, I. Tsukada, T. Yamamoto, K. Uchinokura, Phys. Rev. B **64**, 115104 (2001)
25. D.J. Singh, Phys. Rev. B **61**, 13397 (2000)
26. C. Mazumda, A.K. Nigam, R. Nagarajan, L.C. Gupta, C. Godart, G. Chandra, R. Vijayaraghavan, Phys. Rev. B **54**, 6069 (1996)
27. C. Mazumda, R. Nagarajan, A.K. Nigam, K. Ghosh, S. Ramakrishnan, L.C. Gupta, B.D. Padalia, Physica B **339**, 216 (2003)
28. H. Ohno, H. Munekata, T. Penney, S. von Molnár, L.L. Chang, Phys. Rev. Lett. **68**, 2664 (1992)
29. X.G. Luo et al., in preparation
30. H. Roth, W.D. Straub, W. Bernard, J.E. Mulhern, Phys. Rev. Lett. **11**, 328 (1963)
31. B.C. Sales, R. Jin, K.A. Affholter, P. Khalifah, G.M. Veith, D. Mandrus, Phys. Rev. B **70**, 174419 (2004)
32. H. Yamada, S. Takada, J. Phys. Soc. Jpn **34**, 51 (1973)